

Exploring Λ - and Ξ -triton correlation functions in heavy-ion collisions

Faisal Etminan*

*Department of Physics, Faculty of Sciences,
University of Birjand, Birjand 97175-615, Iran and
Interdisciplinary Theoretical and Mathematical Sciences
Program (iTHEMS), RIKEN, Wako 351-0198, Japan*

(Dated: February 10, 2025)

The Λ - and Ξ -triton(t) momentum correlation functions, to be measured in high-energy heavy-ion collisions, are explored. Mainly, STAR detector acquired data provides an opportunity to explore the Λt correlation function. The Λt correlation functions are calculated using an isle-type and spin-averaged Λt potential, also, its sensitivity to changes in potential strength has also been investigated. Besides, even though there is no experimental data on the Ξ -triton interaction yet, I constructed Ξt potentials based on the first principles HAL QCD and Nijmegen extended soft-core (ESC08c) model of spin- and isospin averaged ΞN interactions in single-folding potentials (SFP) approach. Then, the Ξt correlation functions are calculated for these two modern potentials as well as for Nijmegen hard-core model D (NHC-D) ΞN potential. The numerical results predict that, with good measurement resolution, it might be possible to recognize different potentials with a correlation function at relatively small source sizes, i.e., $R = 1 - 3$ fm.

I. INTRODUCTION

New measurements by the STAR (Solenoidal Tracker at RHIC) Collaboration at RHIC (Relativistic Heavy Ion Collider) shows a significant increase in the Λ binding energy of the hypertriton [1], in fact some of the past values have been called into question [2]. Therefore, the accurate measurements of Λ binding energies of heavier hypernuclei than the hypertriton

* fetminan@birjand.ac.ir

are supposed to make progress our knowledge about the Λ interactions by heavier nuclei.

The ${}^4_{\Lambda}H$ nucleus, a bound state of a Λ hyperon and a tritium core, is an isotope of the hydrogen. It was observed in the primary helium bubble chamber and nuclear emulsion experiments [3]. So far the binding energy of ${}^4_{\Lambda}H$ is measured by different experimental techniques such as the emulsion technique [3], decay-pion spectroscopy in electron scattering [4], high-resolution decay-pion spectroscopy by A1 Collaboration at the Mainz Microtron MAMI, Germany [5] and very recently, it is measured in Au+Au collisions at $\sqrt{s_{NN}} = 3$ GeV by the STAR Collaboration [1, 6].

Since studying YN interactions by the classical scattering experiments is challenging, recent progress in theoretical and experimental techniques in heavy-ion reactions at relativistic energies provide a unique opportunity to explore YN interactions through measuring two-particle correlations [7, 8] and production of light hypernuclei [6]. The first measurement of Λp and Λd correlation, which is done by STAR Collaborations with $\sqrt{s_{NN}} = 3$ GeV Au+Au collisions [9], shed light on both YN two-body and YNN three-body interactions [8, 10–12], which is crucial for understanding neutron star properties. The correlation functions for some hadron-deuteron systems are explored theoretically, such as pd [11, 13, 14], K^-d [12, 14], Λd [8, 15], Ξd [16], and ΩNN [17, 18]. Moreover very recently, the momentum correlation between $\Lambda\alpha$ [19], $\Xi\alpha$ [20], $\Omega\alpha$ [21] and $\phi\alpha$ [22] have been investigated theoretically.

According to the above discussion, it is desirable to predict the Λt momentum correlation functions numerically using phenomenological potentials to be compared by expected measuring Λt correlations function by STAR in the relativistic heavy ion collisions [1] as an independent source of information.

In addition, I explored the formation possibility of $\Xi-t$ system by evaluating its momentum correlation functions applying the effective folding $\Xi-t$ potentials. However, no experimental results or observations have been reported about $\Xi-t$ system so far, but evidence from femtoscopic measurements for an attractive Ξ^-p interaction [23] have triggered significant motivation to investigate Ξ hypernuclei theoretically [24–26]. Therefore. in this work, I constructed a three Gaussian (3G) and a Woods-Saxon (WS) type form for Ξt potential based on the first principles HAL QCD [27] and Nijmegen extended soft-core (ESC08c) [28] model of ΞN interactions, respectively. The Ξt potentials are obtained in the single-folding potentials (SFP) approach by using the corresponding spin- and isospin averaged ΞN interactions. Then the relevant Ξt momentum correlation functions are calculated by employing

these two modern Ξt potentials and another potential built based on phenomenological Nijmegen hard-core model D (NHC-D) ΞN potential which is taken from the literature [29].

Since the present work is an exploratory study, it is done on a simple technical level. Actually, it provide an illustration for what can be expected from measuring Yt correlations. Indeed, in order to analyze actual data of Yt correlations, full-fledged and high precision approach of the Yt system is desired.

The paper is structured as follows: In Sec. II, the employed potentials in this work, i.e., the effective two-body Λt and Ξt potentials, are described, and some properties are discussed. The correlation function results by Koonin-Pratt (KP) formula [30] are given in Sec. III and the relevant discussions about the results also presented there. I summarize and conclude my work in Sec. IV.

II. EFFECTIVE TWO-BODY Λt AND Ξt POTENTIALS

For Λt potential, Kurihara's isle-type potential is employed [31]. That is extracted from Dalitz's hard core ΛN interaction and has a two-range Gaussian form [32]. The strength of Λt potential is tuned in such a way as to reproduce the experimental ground state energy of ${}^4_{\Lambda}H$, $E = -2.04(4)$ MeV for the singlet (S) Λt state [3] and the first excited state energy, $E = -0.99(4)$ MeV for the triplet (T) Λt state [24, 33]. The $U_{\Lambda t}(r)$ potential between t and Λ is given by [29]

$$U_{\Lambda t}(r) = \frac{1}{4}V_{\Lambda t}^S(r) + \frac{3}{4}V_{\Lambda t}^T(r) = \quad (1)$$

$$359.2 \exp\left[-\left(\frac{r}{1.25}\right)^2\right] - 324.9 \exp\left[-\left(\frac{r}{1.41}\right)^2\right],$$

this Isle potential has a two-range Gaussian form with the central repulsion and the long range attraction and it is shown in Fig. 1.

Furthermore, the new Λ binding energies measurements, performed for the ${}^4_{\Lambda}H$ (0^+) state with respect to the ${}^3H + \Lambda$ mass are, $2.12(1)_{\text{stat.}}(9)_{\text{syst.}}$ MeV [4], $2.157(5)_{\text{stat.}}(77)_{\text{syst.}}$ MeV by A1 Collaboration [5] and $2.22(6)_{\text{stat.}}(14)_{\text{syst.}}$ MeV by the STAR Collaboration [1]. Since the new measurements (especially by the STAR Collaboration) show a significant enhancement in the Λ binding energy of the hypertriton and ${}^4_{\Lambda}H$ hypernuclei, and also to check the sensitivity of the correlation function to the nature of Λt interaction, the strengthened

potential, $U_{\Lambda t}^+$ is defined as

$$U_{\Lambda t}^+(r) = 1.2 U_{\Lambda t}(r). \quad (2)$$

The strength of the original (old) potential in Eq. (1) is increased by 20 percent. To compare with $U_{\Lambda t}$ the behavior of this potential is depicted in Fig. 1 as function of the distance between t and Λ . The scattering length, effective range and binding energy of the Λt system for different potentials are summarized in Table I.

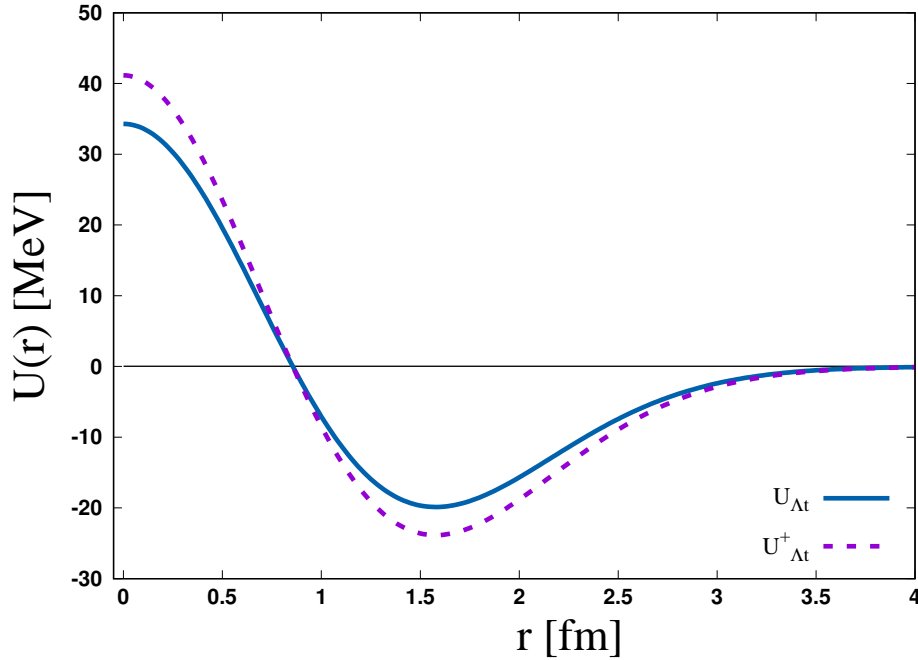


FIG. 1: The spin averaged Λt potentials, $U_{\Lambda t}(r)$, as functions of distance between Λ and triton. $U_{\Lambda t}$ (solid blue line) is given by Eq. (1) and $U_{\Lambda t}^+ = 1.2 U_{\Lambda t}$ (dotted violet line) simulates a 20 percent increment in Λt interaction. The $U_{\Lambda t}$ is taken from Ref. [29].

TABLE I: Scattering length a_0 , effective range r_0 and binding energy B_Λ for Λt system.

The potential $U_{\Lambda t}(r)$ is taken directly from Ref. [29].

Model	a_0 (fm)	r_0 (fm)	B_Λ (MeV)
$U_{\Lambda t}(r)$	5.9	2.3	1.27
$U_{\Lambda t}^+(r)$	4.6	2.1	2.57

In the case of Ξt system, the following folding potential [34, 35], taken from Ref. [29], has

been used,

$$U_{\Xi t}(r) = \sum_{i=1}^3 c_i e^{-(r/d_i)^2}, \quad (3)$$

with the parameters specified in Table II. $U_{\Xi t}(r)$ is built by folding an effective ΞN potential with the triton density distribution function $\rho(r')$ [29, 35],

$$U_{\Xi t}(r) = \int d\mathbf{r}' \rho(r') \bar{V}_{\Xi-N}(\mathbf{r} - \mathbf{r}'), \quad (4)$$

where r is the distance of Ξ^- from the center-of-mass of the triton. The nucleon density in the triton is evaluated from a harmonic oscillator model,

$$\rho(r) = 3 \left(\frac{3\beta}{2\pi} \right)^{3/2} \exp\left(-\frac{3}{2}\beta r^2\right), \quad (5)$$

$\beta = 0.386 \text{ fm}^{-2}$ is the strength of harmonic oscillator that reproduces the matter root-mean-square (rms) radius 1.61 fm which is measured in electron scattering experiments from light nuclei [36]. The effective potential $\bar{V}_{\Xi-N}$ is approximated from the isospin-spin averaged $\Xi^- N$ interaction,

$$\bar{V}_{\Xi-N} = \frac{1}{8} V_{\Xi^- p}^{1S_0} + \frac{3}{8} V_{\Xi^- p}^{3S_1} + \frac{1}{8} V_{\Xi^- n}^{1S_0} + \frac{3}{8} V_{\Xi^- n}^{3S_1}, \quad (6)$$

the two-body potential $V_{\Xi-N}$ between Ξ^- and N are Shinmura's potential [29] which is based on the NHC-D potential [37, 38]. The low-energy data derived with $U_{\Xi t}(r)$ indicates no bound or resonant state. But, if we switch on the Coulomb interaction, the bound state 0.14 MeV appears. Therefore, this is a Coulomb-assisted bound state.

In the following, the ESC08c and the HAL QCD ΞN potentials which are used to find the effective single-folding potential of Ξt is described. The ESC08c Nijmegen ΞN potential function consists of local central Yukawa-type potentials with attractive and repulsive terms [28, 39],

$$V_{\Xi N}^{ESC08c}(r) = -A \frac{\exp(-\mu_A r)}{r} + B \frac{\exp(-\mu_B r)}{r}. \quad (7)$$

where the low-energy data and the parameters of these models are given in Table I of Ref. [39].

For ΞN HAL QCD potential, the concrete parametrizations, are taken straight from Ref. [27] at the imaginary-time slices $t/a = 11, 12, 13$ where $a = 0.0846 \text{ fm}$ is the lattice spacing. Sasaki et al. in Ref. [27] clearly treated $\Lambda\Lambda - \Xi N$ interactions by the HAL QCD coupled-channel formalism [40, 41]. The S-wave ΞN interactions is classified in four channels

$^{11}S_0$, $^{31}S_0$, $^{13}S_1$ and $^{33}S_1$. Here, same as Ref. [27], the spectroscopic notation $^{2I+1,2S+1}S_J$ is employed where I, S and J indicate the total isospin, the total spin, and the total angular momentum, respectively.

For phenomenological applications, the lattice QCD potential was fitted by analytic functional forms composed of multiple Gaussian and Yukawa functions. The Gauss functions set out the short-range part of the potential and Yukawa functions describe the meson exchange picture at medium to long-range distances

$$V_{\Xi N}(r) = \sum_{i=1}^3 \alpha_i e^{-r^2/\beta_i^2} + \lambda_2 [\mathcal{Y}(\rho_2, m_\pi, r)]^2 + \lambda_1 \mathcal{Y}(\rho_1, m_\pi, r), \quad (8)$$

where the values of the parameters $\alpha_{1,2,3}$, $\beta_{1,2,3}$, $\lambda_{1,2}$ and $\rho_{1,2}$ are given in Table 4 of Ref [27]. $m_\pi \simeq 146$ MeV is the pion mass that was measured on the lattice. The form factor \mathcal{Y} defines Yukawa function

$$\mathcal{Y}(\rho, m, r) \equiv \left(1 - e^{-\frac{r^2}{\rho^2}}\right) \frac{e^{-mr}}{r}. \quad (9)$$

Since the $\Xi + t$ system required to show a clear Ξ -core structure, I employ approximately reliable expressions for spin- and isospin dependence of ΞN interaction to s -shell (the core nucleons and the Ξ are in S-wave states). Therefore, in these approximations, the effective ΞN interactions can be obtained by averaging on the spin- and isospin components [42, 43]

$$\bar{V}_{\Xi N} \simeq \frac{\left(V_{\Xi N}^{11S_0} + 3V_{\Xi N}^{31S_0} + 3V_{\Xi N}^{13S_1} + 9V_{\Xi N}^{33S_1}\right)}{16}. \quad (10)$$

In Fig. 2, I compare ΞN potential for (a) the ESC08c model and (b) the HAL QCD at $t/a = 12$ [27]. The statistical errors are not shown in Fig. 2(b), but are considered in my calculations.

Figure 2 reveals a qualitative difference between (a) and (b). Therefore, it is interesting to find out how these differences are embodied in the low energy properties of Ξt systems.

According to the behaviour of the obtained single-folding potentials $U_{\Xi t}(r)$ in Fig. 3, two different analytic functional forms is chosen for fitting. The $U_{\Xi t}$ potentials obtained based on the HAL potentials are fitted by the three-Gaussian functions as given by Eq. (3), and the other one built based on the ESC08c model is fitted by the following Wood-Saxon form (inspired by common Dover-Gal model of potential [44])

$$V_{\Xi t}^{fit}(r) = -V_0 \left[1 + \exp\left(\frac{r - R_c}{t}\right)\right]^{-1}, \quad (11)$$

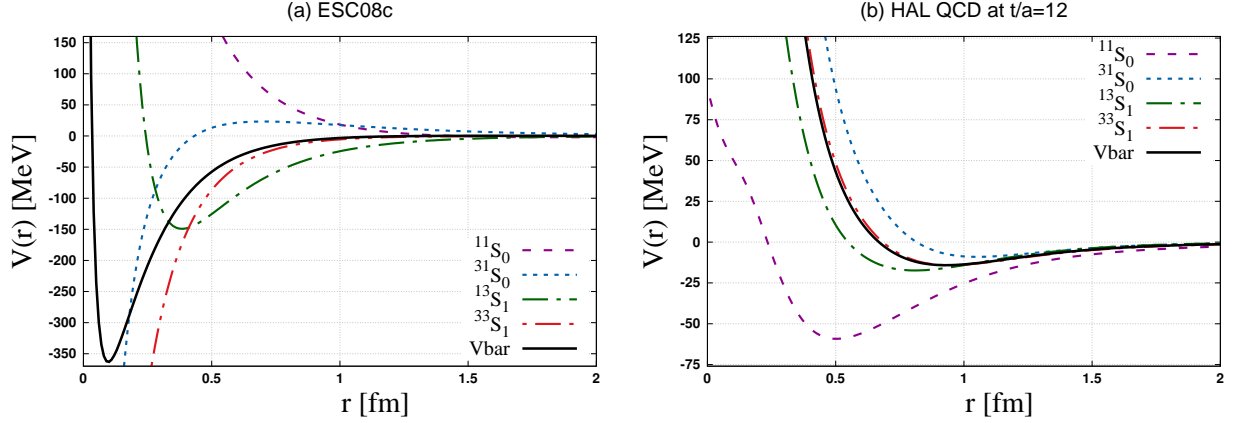


FIG. 2: (a) ESC08c and (b) HAL QCD ($t/a = 12$) ΞN potentials in $^{11}S_0$, $^{31}S_0$, $^{13}S_1$ and $^{33}S_1$ channels. The corresponding scattering phase shifts for each channel are given in Ref. [25]. The solid black line, which is labeled by V_{bar} , shows the spin- and isospin averaged potential, $\bar{V}_{\Xi N}$ in Eq. (10).

where V_0 is depth parameter, $R_c = r_c A^{1/3}$ the radius of the nucleus (with the mass number $A = 3$ for triton) and t the surface diffuseness. In a nucleus, the R_c is measured from the center to a point where the density falls to around half of its value at the center. The WS fit for the Ξt potential is constructed for the interval $r \gtrsim 1.6$ fm [45]. This range is chosen according to the rms radii of triton from experimental measurements.

The binding energy and scattering observables for Λ (Ξ) - t systems are obtained by solving two-body Schrödinger equation using the fitted $U_{Yt}(r)$ potentials (plotted in Figs. 1 and 3) as the input. In our numerical calculations, the mass of Λ , $m_\Lambda = 1115.683$ MeV is taken from the PDG [46], the mass of triton $m_t = 2808.921$ MeV is from CODATA [47] and the mass of Ξ is considered to be $m_\Xi = 1318.07$ MeV. The results for scattering length, effective range, and binding energy of the Ξt are given in Table II. We found that none of the potentials of the HAL $t/a = 11, 12$ and 13 support bound states. Only for the NHC-D and ESC08c models, we have a possibility of a shallow bound state with the binding energies of 0.14 and 0.30 MeV with respect to the $\Xi + t$ threshold.

Moreover, the relevance Yt phase shifts (δ/π) as functions of the relative momentum ($q = \sqrt{2\mu E}$ where μ is the reduced mass of Yt system) is shown in Fig. 4. The obtained phase shifts shows attractive behavior for all interactions. Low-energy part of Yt phase shifts in Fig. 4 defines scattering length a_0 and effective range r_0 employing the effective

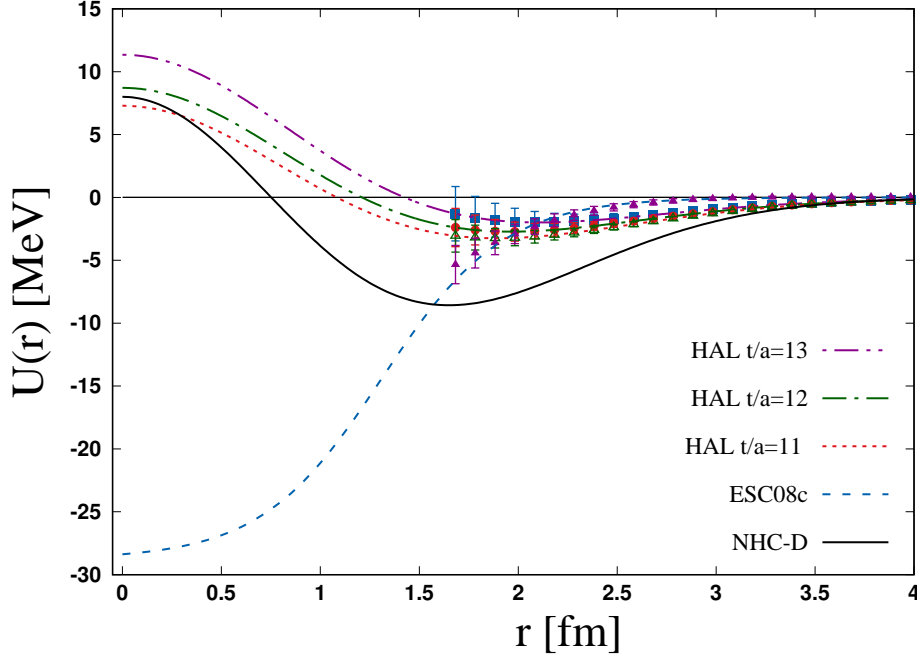


FIG. 3: The spin- and isospin averaged single-folding potentials $U_{\Xi t}$ in Eq. (4) as functions of distance between Ξ and triton. The first three based on HAL QCD Ξ - N potentials at $t/a = 13$ (dash-dot-dotted magenta line), $t/a = 12$ (dash-dotted green line), and $t/a = 11$ (dotted red line). The last two $U_{\Xi t}$, i.e., ESC08c (dashed blue line) and NHC-D (solid black line) are constructed by using the Nijmegen extended soft-core and hard-core models, respectively. The folding NHC-D potential is taken from Ref. [29] as given by Eq. (3). The fit range is taken to be $r \gtrsim 1.6$ fm.

range expansion (ERE) formula,

$$q \cot \delta = -\frac{1}{a_0} + \frac{1}{2}r_0q^2 + \mathcal{O}(q^4). \quad (12)$$

The numerical results for $U_{\Lambda t}$ in Eq. (1), $U_{\Lambda t}^+$ in Eq. (2) and Ξt folding potential in Eq. (3), are listed in table I.

Hiyama et al. in Ref. [25] calculated the binding energy of $NNN\Xi$ states by a high precision variational approach, the Gaussian Expansion Method. They found for ΞNNN system in ESC08c potential, the state in $(T, J^\pi) = (0, 0^+)$ is unbound with respect to $\Xi + {}^3H/{}^3He$ threshold, while the states in $(T, J^\pi) = (0, 1^+), (1, 0^+)$ and $(1, 1^+)$ are bound by 10.20, 3.55 and 10.11 MeV, respectively. While with HAL QCD ΞN potential they found that a possibility of a shallow bound state with the binding energies of 0.63 ($t/a = 11$), 0.36 ($t/a = 12$), 0.18 ($t/a = 13$) MeV with respect to the $\Xi + {}^3H/{}^3He$ thresh-

old. Since we used the spin- and isospin averaged ΞN interaction to build the Ξt potential, our results are some how different with GEM methods [25], but the general behaviours are in agreement.

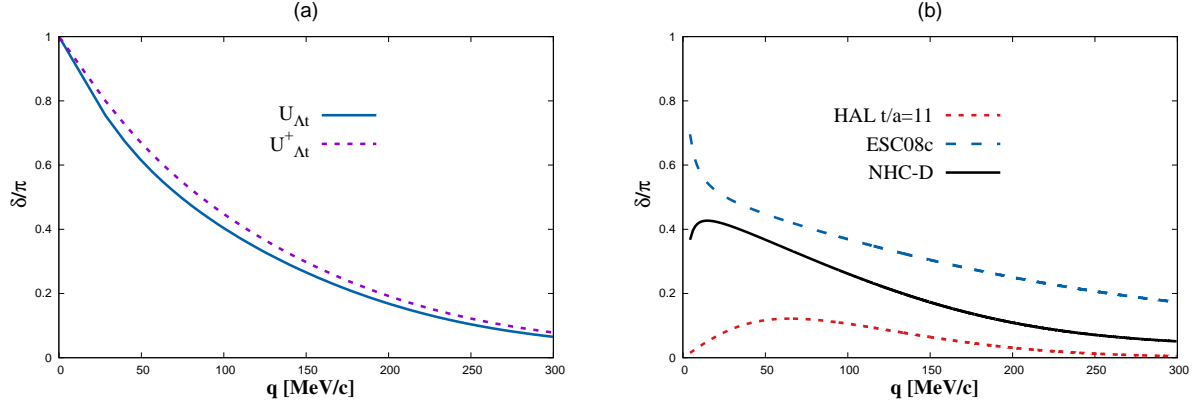


FIG. 4: The normalized phase shifts as functions of the relative momentum q (a) for Λt using $U_{\Lambda t}$ (solid blue line), $U^+_{\Lambda t}$ (dotted violet line); and (b) for Ξt employing $U_{\Xi t}$ based on the HAL QCD $t/a = 11$ (dotted red line), the ESC08c (dashed blue line) and NHC-D (solid black line) model of potentials.

TABLE II: The fit parameters of Ξt potentials, c_i (in MeV) and d_i (in fm) in Eq. (3); V_0 (in MeV), r_c (fm) and t (in fm) in Eq. (11), and the corresponding low-energy parameter, scattering length a_0 (in fm), effective range r_0 (in fm) and binding energy $B_{\Xi t}$ (in MeV) are given for NHC-D, ESC08c and HAL QCD potentials. The binding energy by including Coulomb interaction is given between parentheses, it implies that Ξt system could be a Coulomb-assisted bound state [25, 26].

Model-3G	c_1	d_1	c_2	d_2	c_3	d_3	a_0	r_0	$B_{\Xi t}$
NHC-D	103.67	1.362	-51.57	1.568	-44.10	1.610	-114.0	3.1	-(0.14)
HAL $t/a = 11$	29.3	0.56	-20.5	0.32	-1.5	0.17	-2.2	6.1	-
HAL $t/a = 12$	29.2	0.56	-19.1	0.33	-1.4	0.17	-1.6	7.5	-
HAL $t/a = 13$	29.2	0.56	-16.7	0.33	-1.2	0.17	-1.0	11.5	-
WS	V_0		r_c		t		a_0	r_0	$B_{\Xi t}$
ESC08c	28.8		0.90		0.3		64.2	1.8	-(0.30)

III. CORRELATION FUNCTION RESULTS AND DISCUSSION

The two-particle correlation produced in a collision [7, 30, 48–50] presents valuable information about the space-time evolution of the particle-emitting source and final state interactions entail hyperons [51]. The Yt correlation function is given in terms of the two-particle distribution $N_{Yt}(\mathbf{k}_Y, \mathbf{k}_t)$ normalized by the product of the single particle distributions, $N_Y(\mathbf{k}_Y) N_t(\mathbf{k}_t)$,

$$C(\mathbf{k}_Y, \mathbf{k}_t) \equiv \frac{N_{Yt}(\mathbf{k}_Y, \mathbf{k}_t)}{N_Y(\mathbf{k}_Y) N_t(\mathbf{k}_t)}, \quad (13)$$

where the \mathbf{k}_Y and \mathbf{k}_t are the momentum of particle Y and triton. In the experiments, correlation function is measured by

$$C(q) = \mathcal{N} \frac{A(\mathbf{q})}{B(\mathbf{q})} = \int 4\pi r^2 dr S(\mathbf{r}) \left| \Psi_{Yt}^{(-)}(\mathbf{r}, \mathbf{q}) \right|^2, \quad (14)$$

that is equivalent to Eq. (13). Where $\mathbf{q} = (m_Y \mathbf{k}_Y - m_t \mathbf{k}_t) / (m_Y + m_t)$ is the relative momentum, and $A(\mathbf{q})$ is the distribution of q with both particles from the same event, $B(\mathbf{q})$ is for two particles from different events, and \mathcal{N} is the normalization factor. The right-hand side of Eq. (14) is known as by the Koonin-Pratt (KP) formula [30]. $S(r) = \exp(-r^2/4R^2) / (2\sqrt{\pi}R)^3$ with source size R is known as the source function, which defines the distribution of the relative distance of particle pairs, and is assumed to be spherical and static Gaussian in my calculations. $\Psi_{Yt}^{(-)}$ is the relative wave function of the particle pairs that can be obtained straightforwardly by solving a two-body Schrödinger equation for a given Yt potential.

The Λt correlation functions for three different source sizes, $R = 1, 3$ fm and 5 fm using $U_{\Lambda t}$ and $U_{\Lambda t}^+$ are shown in Fig. 5. The sizes of the sources have been chosen according to the sizes that are usually people used in the exploration of two-hadron correlation functions [19–21]. The particular dip shape can be observed at small source size $R = 1$ fm, that is conventional in the bound state of system near the threshold [19]. Moreover, Fig. 5 for $R = 1$ fm shows the results for all cases of two potentials are different at low momentum $q \lesssim 100$ MeV/c. According to Fig. 1 for $R = 1$, in the low momentum region fm, the $U_{\Lambda t}$ potential model, is more attractive than $U_{\Lambda t}^+$ potential, thus it gives enhancement of $C_{\Lambda t}$, i.e., The $C_{\Lambda t}$ function suppressed due to the strengthening of the repulsive core part in $U_{\Lambda t}^+$ potential. Nevertheless, with the increase of the source size, the difference between the $C_{\Lambda t}(q)$ s decreases until they are almost identical for $R = 5$ fm. As a consequence, the future

measurements of Λt correlation functions in the relatively low momentum region with small radius of the sources, can be used as a probe to study the Λt interaction in dense matter.

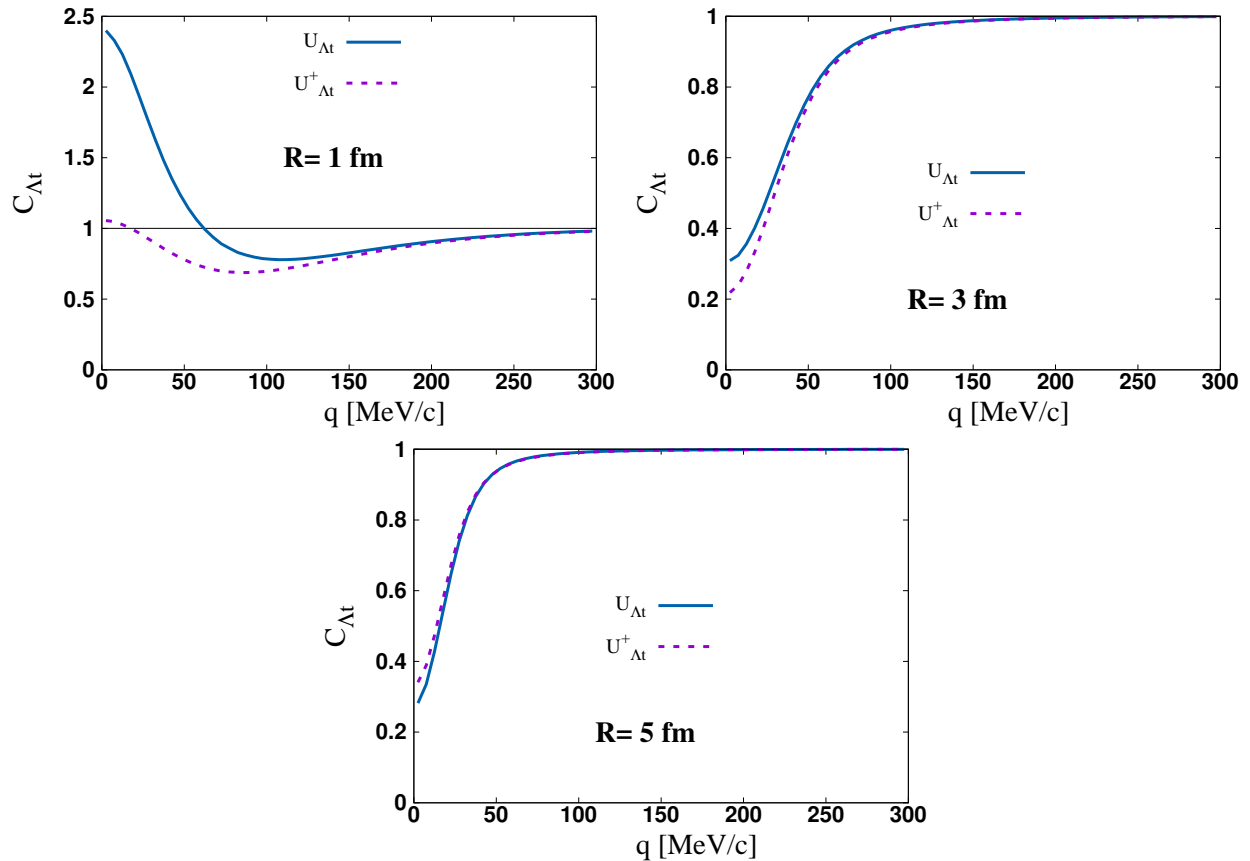


FIG. 5: The spin averaged Λt correlation functions using $U_{\Lambda t}$ (solid blue line), $U_{\Lambda t}^+$ (dotted violet line) for three different source sizes: $R = 1, 3$ and $R = 5$ fm.

The Ξt correlation functions using the HAL QCD $t/a = 11$, ESC08c and NHC-D models of potentials for the three different source sizes are presented in Fig. 6. In this case, the Coulomb potential is also included. It is seen a substantial enhancement in Ξt correlation at low momentum region. That implies a relatively large scattering length (effective range) value for ESC08c, NHC-D (HAL) models of potentials (see table II) and the Coulomb attraction. In order to see the effect of strong interaction, also, the pure Coulomb potential is plotted in Fig. 6. However, with good measurement resolution, it might be possible to recognize different potentials with a correlation function with source size, $R = 1 - 3$ fm. Specifically, $\Xi^- t$ correlation functions are enhanced at the small source and suppressed at the significant source analogous to the pure Coulomb calculation. Moreover, the difference between Ξt correlation function and pure Coulomb result, which is embodied as a dependency

of the correlation function on the size of the source, it implicitly implies the existence of a Coulomb-assisted bound state [20].

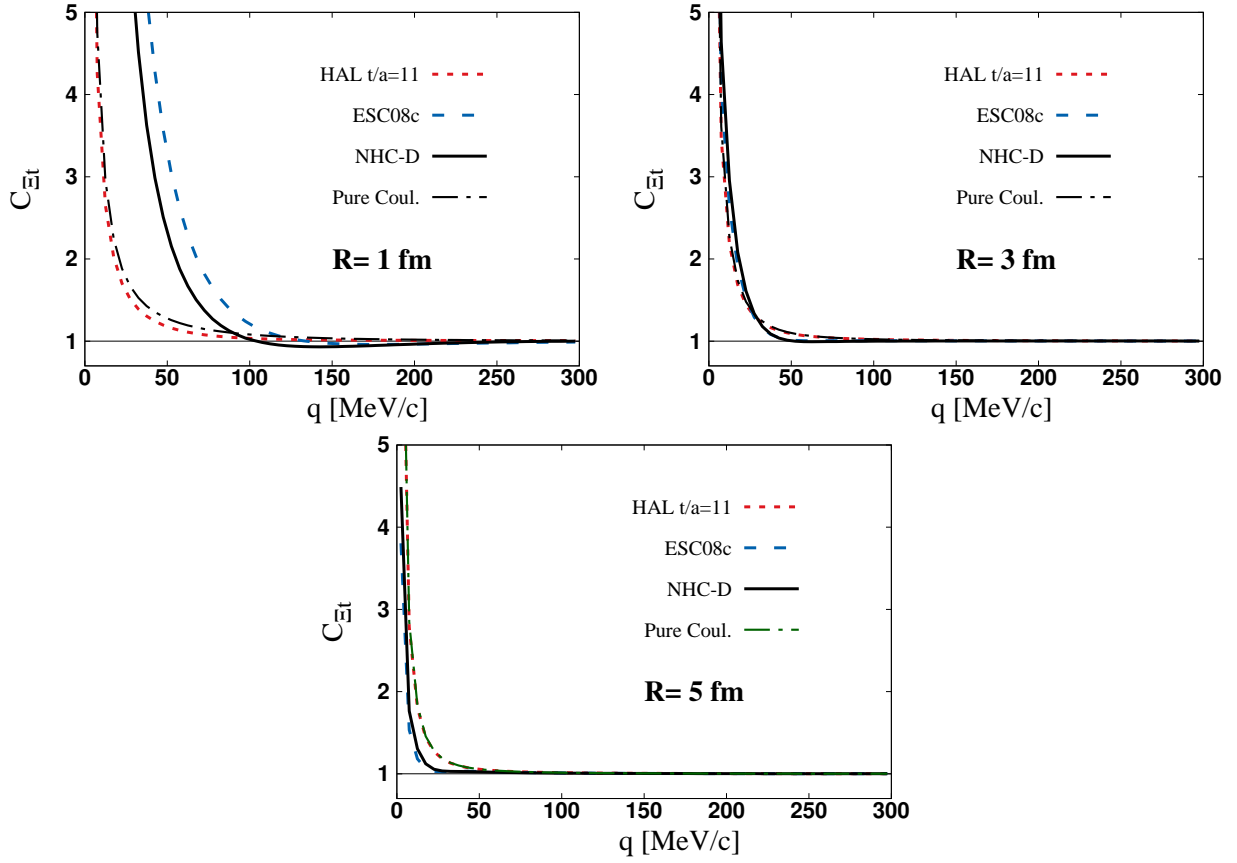


FIG. 6: The spin- and isospin averaged Ξ^-t correlation functions using the HAL QCD $t/a = 11$ (dotted red line), ESC08c (dashed blue line) and NHC-D (solid black line) $U_{\Xi t}$ potentials for three different source sizes: $R = 1, 3$ and $R = 5$ fm, when the Coulomb interaction is switched on. For comparison, the pure Coulomb result, where the strong interaction is switched off, is presented by the dash-dotted green line.

IV. SUMMARY AND CONCLUSIONS

In this exploratory study, Λ and Ξ -triton correlation functions in heavy-ion collisions were predicted. They can be measured in the STAR detector at RHIC [1] by employing the femtoscopy technique.

For Λt two-body potential, Kurihara's isle-type potential [31], that is extracted from Dalitz's hard core ΛN interaction was used. The strength of Λt potential was tuned in such

a way as to return the experimental ground state energy of ${}^4_{\Lambda}H$ [3, 33]. In addition, since the new measurements show a relatively significant increase in the Λ binding energy of the hypertriton and ${}^4_{\Lambda}H$ hypernuclei [1, 4, 5], I also performed the calculations with an increased strength of Λt potential by about twenty percent.

Moreover in the case of Ξt two-body potential, because there is no experimental measurement on the Ξ - t interaction yet, I presented a three Gaussian and a Woods-Saxon type form for Ξt potential based on the first principles HAL QCD and ESC08c model of ΞN interactions, respectively. The Ξt potentials were obtained in the SFP approach by using the corresponding spin- and isospin averaged ΞN interactions. In addition, another Ξt potential built based on Nijmegen hard-core model D (NHC-D) ΞN potential which is taken from the literature [29], was examined. The ESC08c and NHC-D models of ΞN interactions returned the large scattering length without a bound state (a shallow Coulomb-assisted bound state) for the Ξt system.

Employing these obtained Yt potentials, correlation functions were calculated using the KP formula for three different source sizes, $R = 1, 3$ fm and 5 fm, where the choice was motivated by values suggested by analyses of measurements of the two-hadron correlation function in pp collisions and heavy ion collisions [19, 20]. The numerical results suggested that, with good measurement resolution, it might be possible to recognize different potentials with a correlation function at relatively small source sizes, i.e., $R = 1 - 3$ fm. It is remarkable that the KP formula in Eq. (14) is accurate under the condition that two correlated particles can be treated as point-like objects. The source size of the composite particle t should be bigger than those with single hadron emissions, for the reason that, there is a probability of t particle formation by the coalescence of three nucleons emitted from the fireball [13, 14, 52]. Therefore, we rather deal with a four-body scattering problem of a three nucleons and a hyperon. In the other hand, a formation of triton and production of Λt correlation arise at same time. Essentially, this mechanism must be taken into account in future studies and it is beyond the scope of this paper.

In conclusion, the numerical results of this work suggest that measurements of the Λt momentum correlation function in heavy-ion collisions [1, 6] look indeed very promising. Particularly, collected data by the STAR detector from Au+Au collisions at a center-of-mass energy of $\sqrt{s_{NN}} = 3$ GeV provide an opportunity to study the Λt correlation function.

ACKNOWLEDGEMENT

I am grateful to the authors and maintainers of "Correlation Analysis tool using the Schrödinger Equation" (CATS) [53], a modified version of which is used for calculations in this exploratory study. Discussions during the long-term workshop, HHIQCD2024 at Yukawa Institute for Theoretical Physics (YITP-T-24-02), aroused in me the motivation for this work.

-
- [1] M. Abdallah *et al.*, Measurement of ${}^4_{\Lambda}H$ and ${}^4_{\Lambda}He$ binding energy in Au+Au collisions at $\sqrt{s_{NN}} = 3$ GeV, [Phys. Lett. B **834**, 137449 \(2022\)](#).
 - [2] E. Botta, T. Bressani, and A. Feliciello, On the binding energy and the charge symmetry breaking in $A \leq 16$ Λ - hypernuclei, [Nucl. Phys. A **960**, 165 \(2017\)](#).
 - [3] M. Jurič *et al.*, A new determination of the binding energy values of the light hypernuclei ($A \leq 5$), [Nucl. Phys. B **52**, 1 \(1973\)](#).
 - [4] A. Esser *et al.* (A1 Collaboration), Observation of ${}^4_{\Lambda}H$ hyperhydrogen by decay-pion spectroscopy in electron scattering, [Phys. Rev. Lett. **114**, 232501 \(2015\)](#).
 - [5] F. Schulz *et al.*, Ground-state binding energy of ${}^4_{\Lambda}H$ from high-resolution decay-pion spectroscopy, [Nucl. Phys. A **954**, 149 \(2016\)](#), recent Progress in Strangeness and Charm Hadronic and Nuclear Physics.
 - [6] M. Kozhevnikova and Y. B. Ivanov, [Light Hypernuclei Production in Au+Au Collisions at \$\sqrt{s_{NN}} = 3\$ GeV within Thermodynamic Approach \(2024\)](#), [arXiv:2401.04991 \[nucl-th\]](#).
 - [7] S. Cho, T. Hyodo, D. Jido, C. M. Ko, S. H. Lee, S. Maeda, K. Miyahara, K. Morita, M. Nielsen, A. Ohnishi, *et al.*, Exotic hadrons from heavy ion collisions, [Prog. Part. Nucl. Phys. **95**, 279 \(2017\)](#).
 - [8] E. Garrido, A. Kievsky, M. Gattobigio, M. Viviani, L. E. Marcucci, R. Del Grande, L. Fabbiotti, and D. Melnichenko, $p\Lambda$ and $pp\Lambda$ correlation functions, [Phys. Rev. C **110**, 054004 \(2024\)](#).
 - [9] Y. Hu, [Measurements of \$p - \Lambda\$ and \$d - \Lambda\$ correlations in 3 GeV Au+Au collisions at STAR \(2023\)](#), [arXiv:2401.00319 \[nucl-ex\]](#).

- [10] K. Morita *et al.*, Probing multistrange dibaryons with proton-omega correlations in high-energy heavy ion collisions, [Phys. Rev. C **94**, 031901 \(2016\)](#).
- [11] M. Viviani, S. König, A. Kievsky, L. E. Marcucci, B. Singh, and O. V. Doce, Role of three-body dynamics in nucleon-deuteron correlation functions, [Phys. Rev. C **108**, 064002 \(2023\)](#).
- [12] S. Acharya *et al.* (ALICE Collaboration), Exploring the Strong Interaction of Three-Body Systems at the LHC, [Phys. Rev. X **14**, 031051 \(2024\)](#).
- [13] S. Bazak and S. Mrówczyński, Production of ${}^4\text{Li}$ and p - ${}^3\text{He}$ correlation function in relativistic heavy-ion collisions, [Eur. Phys. J. A **56**, 193 \(2020\)](#).
- [14] S. Mrówczyński and P. Słoń, Hadron-deuteron correlations and production of light nuclei in relativistic heavy-ion collisions, [Acta Phys. Pol. B **51**, 1739 \(2020\)](#).
- [15] J. Haidenbauer, Exploring the Λ -deuteron interaction via correlations in heavy-ion collisions, [Phys. Rev. C **102**, 034001 \(2020\)](#).
- [16] K. Ogata, T. Fukui, Y. Kamiya, and A. Ohnishi, Effect of deuteron breakup on the deuteron- Ξ correlation function, [Phys. Rev. C **103**, 065205 \(2021\)](#).
- [17] L. Zhang, S. Zhang, and Y.-G. Ma, Production of ΩNN and $\Omega\Omega N$ in ultra-relativistic heavy-ion collisions, [Eur. Phys. J. C **82**, 1 \(2022\)](#).
- [18] F. Etminan, Z. Sanchuli, and M. M. Firoozabadi, Geometrical properties of ΩNN three-body states by realistic NN and first principles Lattice QCD ΩN potentials, [Nucl. Phys. A **1033**, 122639 \(2023\)](#).
- [19] A. Jinno, Y. Kamiya, T. Hyodo, and A. Ohnishi, Femtoscopic study of the $\Lambda\alpha$ interaction, [Phys. Rev. C **110**, 014001 \(2024\)](#).
- [20] Y. Kamiya, A. Jinno, T. Hyodo, and A. Ohnishi, [Theoretical study on \$\Xi\alpha\$ correlation function \(2024\)](#), [arXiv:2409.13207 \[nucl-th\]](#).
- [21] F. Etminan, Femtoscopic study of the $\Omega\alpha$ interaction in heavy-ion collisions, [Phys. Rev. C **111**, 014912 \(2025\)](#).
- [22] F. Etminan, [Exploring the \$\phi\$ - \$\alpha\$ interaction via femtoscopic study \(2024\)](#), [arXiv:2410.22756 \[nucl-th\]](#).
- [23] S. Acharya *et al.* (A Large Ion Collider Experiment Collaboration), First observation of an attractive interaction between a proton and a cascade baryon, [Phys. Rev. Lett. **123**, 112002 \(2019\)](#).

- [24] H. Le, J. Haidenbauer, U.-G. Meißner, and A. Nogga, Implications of an increased Λ -separation energy of the hypertriton, *Phys. Lett. B* **801**, 135189 (2020).
- [25] E. Hiyama *et al.*, Possible lightest Ξ hypernucleus with modern ΞN interactions, *Phys. Rev. Lett.* **124**, 092501 (2020).
- [26] E. Hiyama, M. Isaka, T. Doi, and T. Hatsuda, Probing the Ξn interaction through inversion of spin-doublets in $\Xi n \alpha \alpha$ nuclei, *Phys. Rev. C* **106**, 064318 (2022).
- [27] S. Kenji *et al.* (HAL QCD Collaboration), $\Lambda\Lambda$ and $N\Xi$ interactions from lattice QCD near the physical point, *Nucl. Phys. A* **998**, 121737 (2020).
- [28] M. M. Nagels, T. A. Rijken, and Y. Yamamoto, Extended-soft-core baryon-baryon ESC08 model III. $S = -2$ hyperon-hyperon/nucleon interaction (2015), [arXiv:1504.02634 \[nucl-th\]](https://arxiv.org/abs/1504.02634).
- [29] K. S. Myint and Y. Akaishi, Double-Strangeness Five-Body System, *Prog. Theor. Phys.* **117**, 251 (1994).
- [30] A. Ohnishi, K. Morita, K. Miyahara, and T. Hyodo, Hadron-hadron correlation and interaction from heavy-ion collisions, *Nucl. Phys. A* **954**, 294 (2016).
- [31] Y. Kurihara, Y. Akaishi, and H. Tanaka, Effect of Λ -N repulsive core on pionic decay of ${}^5_{\Lambda}\text{He}$, *Phys. Rev. C* **31**, 971 (1985).
- [32] R. Dalitz, R. Herndon, and Y. Tang, Phenomenological study of s-shell hypernuclei with ΛN and ΛNN potentials, *Nucl. Phys. B* **47**, 109 (1972).
- [33] T. O. Yamamoto *et al.* (J-PARC E13 Collaboration), Observation of Spin-Dependent Charge Symmetry Breaking in ΛN Interaction: Gamma-Ray Spectroscopy of ${}^4_{\Lambda}\text{He}$, *Phys. Rev. Lett.* **115**, 222501 (2015).
- [34] G. Satchler and W. Love, Folding model potentials from realistic interactions for heavy-ion scattering, *Phys. Rep.* **55**, 183 (1979).
- [35] F. Etminan and M. M. Firoozabadi, Simple Woods-Saxon type form for $\Omega\alpha$ and $\Xi\alpha$ interactions using folding model, *Chin. Phys. C* **44**, 054106 (2020).
- [36] C. Ciofi degli Atti, Electron scattering by nuclei, *Prog. Part. Nucl. Phys.* **3**, 163 (1980).
- [37] M. M. Nagels, T. A. Rijken, and J. J. de Swart, Baryon-baryon scattering in a one-boson-exchange-potential approach. II. Hyperon-nucleon scattering, *Phys. Rev. D* **15**, 2547 (1977).
- [38] P. M. M. Maessen, T. A. Rijken, and J. J. de Swart, Soft-core baryon-baryon one-boson-exchange models. II. Hyperon-nucleon potential, *Phys. Rev. C* **40**, 2226 (1989).

- [39] H. Garcilazo, A. Valcarce, and J. Vijande, Maximal isospin few-body systems of nucleons and Ξ hyperons, *Phys. Rev. C* **94**, 024002 (2016).
- [40] S. Aoki, B. Charron, T. Doi, T. Hatsuda, T. Inoue, and N. Ishii, Construction of energy-independent potentials above inelastic thresholds in quantum field theories, *Phys. Rev. D* **87**, 034512 (2013).
- [41] F. Etminan, K. Sasaki, and T. Inoue, Coupled-channel $\Lambda_c K^+ - p D_s$ interaction in the flavor SU(3) limit of lattice QCD, *Phys. Rev. D* **109**, 074506 (2024).
- [42] E. Hiyama, Y. Yamamoto, T. Motoba, T. A. Rijken, and M. Kamimura, Light Ξ hypernuclei in four-body cluster models, *Phys. Rev. C* **78**, 054316 (2008).
- [43] H. Le, J. Haidenbauer, U.-G. Meißner, and A. Nogga, $A = 4 - 7$ Ξ hypernuclei based on interactions from chiral effective field theory, *Eur. Phys. J. A* **57**, 1 (2021).
- [44] C. Dover and A. Gal, Ξ Hypernuclei, *Ann. Phys.* **146**, 309 (1983).
- [45] I. Filikhin, R. Y. Kezerashvili, and B. Vlahovic, Folding Procedure for Ω - α Potential, *Few-Body Syst.* **66**, 2 (2024).
- [46] P. A. Zyla and others (Particle Data Group), Review of Particle Physics, *Prog. Theor. Exp. Phys.* **2020**, 083C01 (2020), https://academic.oup.com/ptep/article-pdf/2020/8/083C01/34673740/rpp2020-vol2-2015-2092_18.pdf.
- [47] M. Wang, G. Audi, F. G. Kondev, W. J. Huang, S. Naimi, and X. Xu, The AME2016 atomic mass evaluation (II). Tables, graphs and references, *Chin. Phys. C* **41**, 030003 (2017).
- [48] S. E. Koonin, Proton pictures of high-energy nuclear collisions, *Phys. Lett. B* **70**, 43 (1977).
- [49] S. Pratt, Pion interferometry of quark-gluon plasma, *Phys. Rev. D* **33**, 1314 (1986).
- [50] K. Morita, T. Furumoto, and A. Ohnishi, $\Lambda\Lambda$ interaction from relativistic heavy-ion collisions, *Phys. Rev. C* **91**, 024916 (2015).
- [51] L. Fabbietti, V. M. Sarti, and O. V. Doce, Study of the Strong Interaction Among Hadrons with Correlations at the LHC, *Annu. Rev. Nucl. Part. Sci.* **71**, 377 (2021).
- [52] S. Mrówczyński and P. Słoń, Deuteron-deuteron correlation function in nucleus-nucleus collisions, *Phys. Rev. C* **104**, 024909 (2021).
- [53] D. Mihaylov, V. Sarti, O. Arnold, L. Fabbietti, B. Hohlweger, and A. Mathis, A femtoscopic Correlation Analysis Tool using the Schrödinger equation (CATS), *Eur. Phys. J. C* **78** (2018).